Proceedings of ASME FEDSM'03
4th ASME_JSME Joint Fluids Engineering Conference
Honolulu, Hawaii, USA, July 6-10, 2003

FEDSM2003-45432

Computational Analysis of Turbulent Flow Around A Dimpled and smooth sphere

Khalid N. Alammar

Department of Mechanical Engineering, King Saud University
PO Box 800, Riyadh 11421, Saudi Arabia
+966 (01) 467-6650
+966 (01) 467-6652
alammar@ksu.edu.sa

and

Space Research Institute, King Abdulaziz City for Science and Technology
PO Box 6086, Riyadh 11442, Saudi Arabia
+966 (01) 481-3722
alammar@kacst.edu.sa

ABSTRACT

Steady turbulent flow around a 43-mm diameter smooth sphere and one with 245 round dimples was simulated. The turbulent flow around the sphere was attained by placing a turbulator 9 mm's upstream of the center point. For comparison, the turbulator was also placed around the dimpled sphere. The simulation revealed stable vortical flow structure inside the dimples. A stable vortex pair in the wake region was predicted in both cases. Predicted separation point over the smooth sphere was further downstream than in the case of dimpled sphere. The predicted drag coefficient for the smooth sphere was 40 % lower than that of the dimpled sphere, which was 0.35. Drag predictions are compared with previously published measurements.

INTRODUCTION

There are many applications involving fluid flow over blunt bodies, and many examples can be seen in sports. A good example at hand is the golf ball, on which numerous investigations have been invested. Prior to the discovery of the effect of dimples, Tait [1] studied physics of golf balls through trajectories. After introducing dimples, studies continued on golf ball aerodynamics. Davies [2], for example, conducted measurements of lift and drag on golf balls using trajectories. Bearman and Harvey [3] used hexagonal and conventional-dimpled golf balls in their comprehensive wind-tunnel measurements of drag and lift on golf balls with various spin rates and Reynolds numbers. Smits and Smith [4] conducted similar measurements, and obtained an aerodynamic model to predict drag and lift over a given range of Reynolds numbers and spin rates. Recently, Kato et al. [5] conducted a numerical study on a spinning and non-spinning golf ball using a laminar flow model. While they aimed to capture drag reduction due to dimples, their results showed a drag increase on the golf ball, as compared to the smooth sphere. The increase in drag with dimples should have been anticipated since the drag decrease in golf balls is due to separation delay promoted by turbulence, which is triggered by dimples. Dimples on golf balls promote turbulence, the fluctuations of which energize the boundary layer, resulting in separation delay, and hence form drag reduction. However, by generating stable vortices and altering local direction of flow, dimples themselves contribute significantly to drag, compared to a smooth sphere under the same freestream flow conditions.

Unlike simulation of Kato et al., which was laminar, in this work, a turbulent flow around a smooth and 245-dimple sphere was simulated. The dimples were 0.6-mm deep and 3.7-mm in diameter. By using a turbulator in both cases, the difference in predicted drag for the smooth and dimpled spheres would be that due to dimples. The turbulator was a 0.2-mm thick, 40-mm diameter torus placed 9 mm's upstream of the center point. The simulation was carried out at $Re = 2x10^5$, corresponding to Ma = 0.2. The results are compared with measurements of Bearman and Harvey [3].

NUMERICAL PROCEDURE

Fluent 6.0 was used as the solver. The simulation was carried out using SIMPLEC [6] and second-order schemes. The linearized equations were solved using the Gauss-Seidel method, in conjunction with an algebraic Multigrid scheme [7]. Spalart-Almaras [8] model was used in the formulation. The SA model was designed for wall-bounded flows, and was shown to give reasonable results involving boundary-layers with adverse pressure gradients. It was chosen for its simplicity (one-equation model), while keeping in mind that the present simulation was merely meant to compare drag coefficients for two similar bodies, and not necessarily predict drag coefficients accurately. The ideal gas and Sutherland's laws were used for density and viscosity calculations, respectively. Gambit was used to construct an unstructured mesh. Two mesh blocks were generated to accommodate the wake region and the remainder of the computational space. A 0.2-mm, 8-layer boundary layer was constructed, and the first row was 0.01-mm high. The mesh consisted of 2,109,935 cells (tetrahedral for the domain and wedges for the boundary layer) [9]. Dimples consisted of 105 cells each. Standard atmospheric conditions and a turbulence viscosity ratio of 0.001 were applied at the far-field boundary. The far field was 20

diameters away from the surface. Smooth surface was assumed. Initial conditions were set to those of the far-field, except for the velocity that was reduced to half the value.

UNCERTAINTY ANALYSIS

There are mainly two sources of uncertainty in CFD simulation, namely modeling and numerical [10]. Modeling uncertainty is approximated through a benchmark solution, and while an experimental validation is not available for the geometrically exact case at hand, an attempt is made to compare results with experimental measurements of a similar case. The numerical uncertainty has two main sources, namely truncation and round-off errors. As was outlined earlier, the discretisation schemes invoked were second-order, which relatively relaxes the requirement of having to reduce the grid size substantially. Round-off error increases with increased number of iterations, and is reduced by increasing significant digits used in the calculations. The number of iterations required for convergence was approximately 2000 in both cases. Further, a double-precision in a 64-bit machine was invoked. Verification of the numerical uncertainty was attained through grid independence that was met with an error of approximately 5 % for both cases.

RESULTS AND DISCUSSION

Y^+ profile at the wall is shown in Figure 1. To avoid crowding, values were plotted every 40 points. The values for both cases are confined between 0 and 5. Hence, and based on law of the wall, [11], the viscous sublayer has been resolved. The dark profile is that of the smooth sphere (baseline). Clearly, the profile for the baseline is fairly smooth, and not as scattered as in the case of dimpled sphere. Y^+ is proportional to shear stress at the wall, which increases while the flow is attached, then drops near separation and remains low in the wake region. Separation and wake regions are associated with relatively low velocities, hence the lower shear stress. Contours of the pressure coefficient are shown in Fig. 2. It is predicted that the separation point for the baseline is further downstream than in the case of dimpled sphere. In part, energy lost to stable vortices inside dimples contributed to the earlier separation. Velocity vectors around a dimple are depicted in Fig. 3. A stable vortex is clearly revealed inside the dimple. The velocity vectors at the middle cross section are depicted in Fig. 4. The flow was fairly symmetric, and a vortex pair is predicted in the wake region. The two vortices are fairly similar. Drag coefficients are shown in Table 1. A 40 % decrease in drag was predicted, which was caused by the presence of dimples. In this study, accuracy of drag prediction was not more important than the relative change in drag brought about by introducing dimples to a smooth sphere. However, compared to the measurements of Bearman and Harvey [3], drag was overestimated. Discrepancy may be attributed to many reasons, including the fact that turbulence was assumed throughout. Early turbulence mixing slows the accelerating fluid (up-hill), resulting in a relative increase in pressure, which in turn, increases drag. At $Re = 2.0x10^5$, flow over a smooth sphere is laminar, and hence a measurement with a turbulator is needed for comparison. The turbulator had no significant effect on the dimpled sphere, as the fluctuations due to dimples were over-shadowing its effect. For assurance, a simulation of the dimpled sphere without the turbulator was conducted, which revealed no change in drag coefficient within the significant digits reported.

CONCLUSIONS AND RECOMMENDATIONS

Steady turbulent flow around a 43-mm diameter smooth sphere and one with 245 round dimples were simulated. The dimples were 0.6-mm deep and 3.7-mm in diameter. The simulation revealed stable vortical flow structure inside the dimples. Predicted separation point over the smooth sphere was further downstream than it was over the dimpled sphere. The predicted drag coefficient for the smooth sphere was 40 % lower than that of the dimpled sphere, which was 0.35. The drag increase due to dimples should be encouraging to investigate new ideas to promote turbulence without a much drag penalty. Analysis is needed for a rotating golf ball, while experimental work is recommended for a turbulent flow around a smooth sphere at $Re = 2.0x10^5$.

ACKNOWLEDGMENTS

This work was conducted at the high-performance computing center at the numerical simulations center (NSC), space research institute, King Abdul Aziz City for Science and Technology, Riyadh, Saudi Arabia, using a Gateway2000 machine. Special Thanks are due to Dr. Turki Al-Saud, director of the institute and Dr. Abdualziz Almadi, assistant director and manager of NSC, both for their generous support. Many thanks are also due to Mr. Harvey Rai for his continuous support as the system administrator at NSC.

REFERENCES

1. Tait, PG, 1890, “Some Points in the Physics of Golf. Part I, “ Nature 42.
2. Davies, J. M., 1949, “The Aerodynamics of Golf Balls, “ Journal of Applied Physics, V. 20, P. 821.
3. Bearman, PW and Harvey, JK, 1976, “Golf ball aerodynamics, “ Aeronautical Quarterly, 27, pp. 112-122.
4. Smits, AJ and Smith, 1994, "A new aerodynamic model of a golf ball in flight," Science and Golf II: Proceedings of the World Scientific Congress of Golf, pp. 340-347.
5. Kato, T, Fujita, T, Ito, Y, Nakahashi, K, and Kohama, Y, 2001, “Computational Analysis of Separated Flow Using Around A Golf Ball Using Unstructured CFD, “ AIAA paper 2001-2569, 15th AIAA Computational Fluid Dynamics Conference, 11-14 June 2001. Anaheim, CA.
6. Vandoormaal, JP and Raithby, GD, 2001, “Enhancements of the SIMPLE Method for Predicting Incompressible Fluid Flows, “ Numerical Heat Transfer. **7**, 147-163, 1984.
7. Fluent 6.0 User’s Guide.
8. Spalart, P and Allmaras, S , 1992, “A One-Equation Turbulence Model for Aerodynamic Flows, “ Technical Report, AIAA-92-0439.
9. Sharov, D and Nakahashi, K, 1998, “Hybrid Prismatic/Tetrahedral Grid Generation for Viscous Flow Applications, “ AIAA Journal, Vol. 36, No. 2.
10. Stern, F, Wilson, R, Coleman, H, and Paterson, E, 1999, “ Verfication and Validation of CFD Simulations, “IIHR Report No. 407, Iowa Institute of Hydraulic Research, College of Engineering, The University of Iowa, Iowa City, IA.
11. Schlichting, H and Gersten, K, “Boundary Layer Theory, 2000, “ 8th edition, Springer.

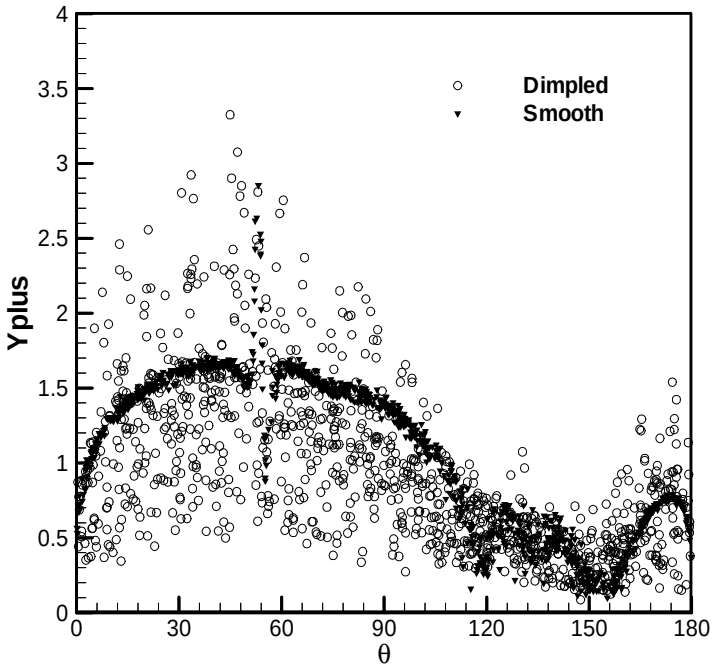

Figure 1: Y+ profile at the wall.

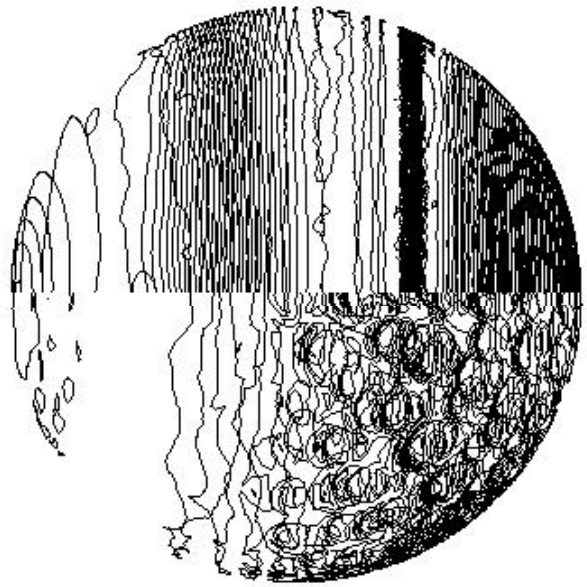

Figure 2: Contours of pressure coefficient at the wall;
(top: smooth, bottom: dimpled)

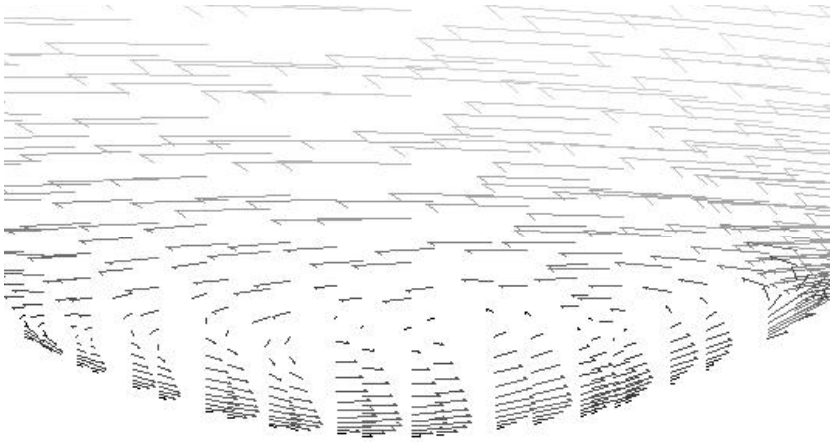

Figure 3: A stable vortex inside a dimple.

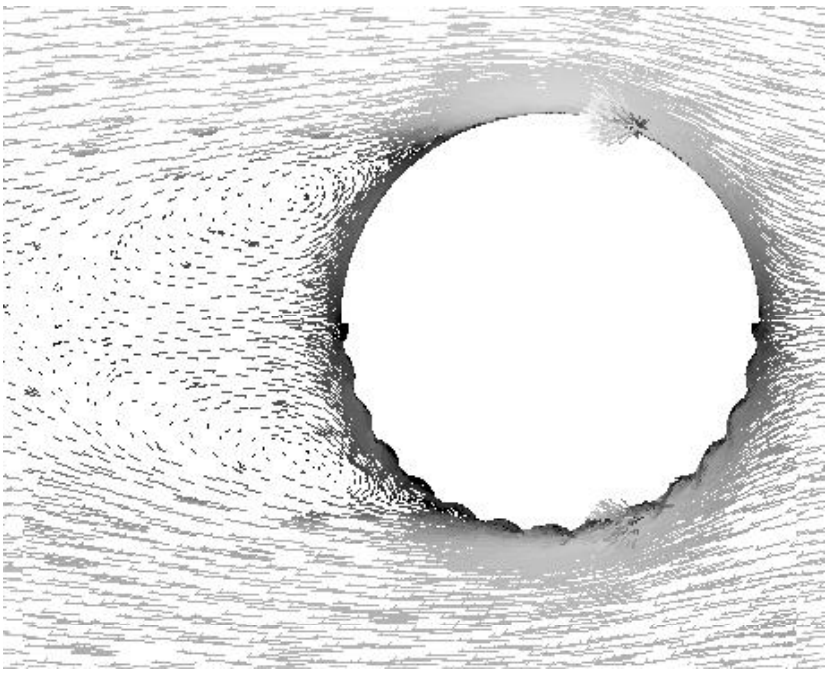

**Figure 4: Velocity vectors at the middle cross section;
(top: smooth, bottom: dimpled)**

Table 1: Drag coefficients.

	Simulation	Measurement
Dimpled Sphere	0.35	0.27
Smooth Sphere	0.21	Blank
Change	- 40 %	Blank